

Upwelling of Atlantic Water along the Canadian Beaufort Sea Continental Slope: Favorable Atmospheric Conditions and Seasonal and Interannual Variations

SERGEI KIRILLOV AND IGOR DMITRENKO

Centre for Earth Observation Science, University of Manitoba, Winnipeg, Manitoba, Canada

BRUNO TREMBLAY

McGill University, Montreal, Quebec, Canada

YVES GRATTON

Institut National de la Recherche Scientifique, Quebec, Quebec, Canada

DAVID BARBER AND SØREN RYSGAARD

Centre for Earth Observation Science, University of Manitoba, Winnipeg, Manitoba, Canada

(Manuscript received 9 November 2015, in final form 17 March 2016)

ABSTRACT

The role of wind forcing on the vertical displacement of the -1°C isotherm and 33.8 isohaline depths was examined based on snapshots of historical (1950–2013) temperature and salinity profiles along the Mackenzie continental slope (Beaufort Sea). It is found that upwelling is correlated with along-slope northeast ($T59^{\circ}$) winds during both ice-free and ice-covered conditions, although the wind impact is more efficient during the ice-free season. One of the most important factors responsible for vertical displacements of isopycnals is sustained wind forcing that can last for several weeks and even longer. It accounts for 14%–55% of total variance in isotherm/isohaline depths, although these numbers might be underestimated. The upwelling and downwelling events are discussed in the context of the interplay between two regional centers of action—the Beaufort high and Aleutian low—that control the wind pattern over the southern Beaufort Sea. The probability of upwelling-favorable wind occurrence is closely related to the sea level pressure difference between these two centers, as well as their geographical positions. The combined effect of both centers expressed as the SLP differences is highly correlated (0.68/0.66 for summer/winter) with occurrences of extreme upwelling-favorable northeast (NE) winds over the Mackenzie slope, although the Beaufort high plays a more important role. The authors also diagnosed the predominant upwelling-favorable conditions over the Mackenzie slope in the recent decade associated with the summertime amplification of the Beaufort high. The upwelling-favorable NE wind occurrences also demonstrate the significant but low (-0.30) correlation with Arctic Oscillation (AO) during both summer and winter seasons, whereas the high correlation with North Pacific index (NPI; -0.52) is obtained only for the ice-covered period.

1. Introduction

Wind-driven upwelling along shelf breaks leads to considerable modification of local water masses and shelfbreak exchanges (e.g., Estrade et al. 2008). In the Arctic this process is often associated with the onshore

transport of warm and relatively salty Atlantic Water (AW) to the continental shelves of the Barents (Falk-Petersen et al. 2015), Laptev (Dmitrenko et al. 2001, 2010), Chukchi (Christensen et al. 2008; Spall et al. 2014), and Beaufort Seas (Carmack and Kulikov 1998; Aagaard and Roach 1990; Pickart et al. 2009; Jackson et al. 2015). The cross-shelf transport of AW can affect vertical heat and salt fluxes with potential implication for the overlying sea ice cover (Polyakov et al. 2010; Barber et al. 2015). On the Beaufort Sea shelf, relatively cold and nutrient-rich Pacific winter waters can be

Corresponding author address: S. Kirillov, Centre for Earth Observation Science, University of Manitoba, Winnipeg MB R3T 2N2, Canada.
E-mail: sergei.kirillov@umanitoba.ca

upwelled, affecting the carbon cycle and biological processes such as primary production (Mundy et al. 2009; Mathis et al. 2012; Pickart et al. 2013a). The southern part of the Beaufort Sea is ice covered and isolated from the atmosphere from October to June suppressing the power input by surface wind to the mixed layer as well as cross-shelf exchange associated with upwelling dynamics (Carmack and Chapman 2003). Note, however, that Williams et al. (2006) showed that strong ice–ocean stress was possible for westward wind at the Mackenzie shelf. Moreover, Williams et al. (2006) and Jackson et al. (2015) reported a maximum vertical water displacement associated with upwelling events in winter, on the same order of magnitude as that reported by Carmack and Kulikov (1998) for the same region during ice-free conditions. Over the Alaskan Beaufort Sea shelf break, Schulze and Pickart (2012) found the strongest upwelling events during the partial ice-covered season, attributing it to more effective wind stress transmittance with freely moving ice keels. The winter upwelling over the Beaufort Sea continental slope can result in reduced vertical stratification of the inner shelf waters. This, in turn, facilitates the formation of Beaufort Sea Winter Water and contributes (if dense enough) to the Arctic cold halocline (Jackson et al. 2015).

Changes in shelf water hydrography associated with upwelling events strongly correlate with the along-slope wind events. In the southern Beaufort Sea, easterly winds are often present associated with two centers of large-scale atmospheric circulation—the Beaufort Sea high to the north and the Aleutian low to the south. The east–west orientation of the continental slope along the Alaskan coastline makes these easterly winds favorable for upwelling during all seasons because of the northward (offshore) Ekman transport of both sea ice and water. In the last few decades, frequent reversals of the atmospheric circulation result in cyclonic sea ice drift in the Beaufort Gyre in all seasons (Lukovich and Barber 2006; Asplin et al. 2009) leading to downwelling-favorable atmospheric conditions instead over the Beaufort continental slope.

The monthly climatology of easterly wind speed has two peaks: one in November when the contrast in air and surface ocean temperature and the baroclinicity is at its highest and one in May when the storm track moves northward (Pickart et al. 2013a). The most intensive individual storms, however, are observed in August (Pickart et al. 2013a), which is consistent with the findings of Serreze and Barrett (2011), who reported the local maximum in anticyclonic winds over the southern Beaufort Sea during summer season. Despite the larger mean easterly wind speed in May and November, the seasonal ice cover considerably modifies the momentum transfer from the surface winds to the surface ocean and

impacts the dynamics of upwelling/downwelling. Depending on wind direction the internal ice stresses resulting from sea ice interactions with the coastline might prevent free drift and suppress the Ekman transport in the surface layer. For instance, Williams et al. (2006) reported a blockade of downwelling-causing ice motion in the Mackenzie Canyon during onshore winds in winter. During August, the transfer of momentum from the surface winds to the ocean and Ekman-driven upwelling can also be constrained by sea ice if the pack ice edge remains shoreward of the shelf break (Carmack and Chapman 2003). Thus, the sea ice retreat, the elongation of the ice-free period (Stroeve et al. 2014), and the associated increase in storm activity (Sorteberg and Walsh 2008; Asplin et al. 2015) suggest more pronounced shelf–basin exchange in the future.

The individual wind-forced upwelling events in the southern Beaufort Sea are well documented based on the long-term mooring records (Carmack and Kulikov 1998; Williams et al. 2006; Pickart et al. 2009) and snapshot oceanographic surveys (Cameron 1953; Garneau et al. 2006; Mundy et al. 2009; Tremblay et al. 2011; Mathis et al. 2012; Sévigny et al. 2015), although a complete assessment of all historical oceanographic data has not been made to date. Over the Alaskan continental slope, the occurrence of upwellings has been studied based only on wind statistics under the assumption that along-slope easterly winds cause the maximum effect on the cross-shelf exchange (Pickart et al. 2013a). Although the occurrence of upwellings over the Mackenzie Beaufort Sea continental slope has been studied based on the northeasterly wind statistics (Williams and Carmack 2015), the validation of upwelling-favorable wind conditions has yet to be demonstrated for this region. In this paper, we analyze all historical temperature and salinity profiles in the southern part of the Canadian Beaufort Sea during 1950–2013 in order to consider the typical atmospheric circulation characterizing the upwelling or downwelling events. We focus on favorable wind patterns that cause upwelling of warmer intermediate AW onto the shelf based on vertical temperature and salinity profiles made over the Mackenzie continental slope. Particularly, we consider the cumulative wind forcing at different time scales on the isotherm and isohaline depth displacement during ice-free and ice-covered seasons and demonstrate the typical SLP patterns corresponding to the extreme water displacements (presumably observed during upwelling and downwelling). We also discuss the relationship between upwelling-favorable wind events—from NCEP reanalysis atmospheric data—and large-scale atmospheric teleconnections (*viz.*, the Arctic Oscillation and North Pacific index) and related atmospheric pressure patterns (*viz.*, the Beaufort Sea high and the Aleutian low).

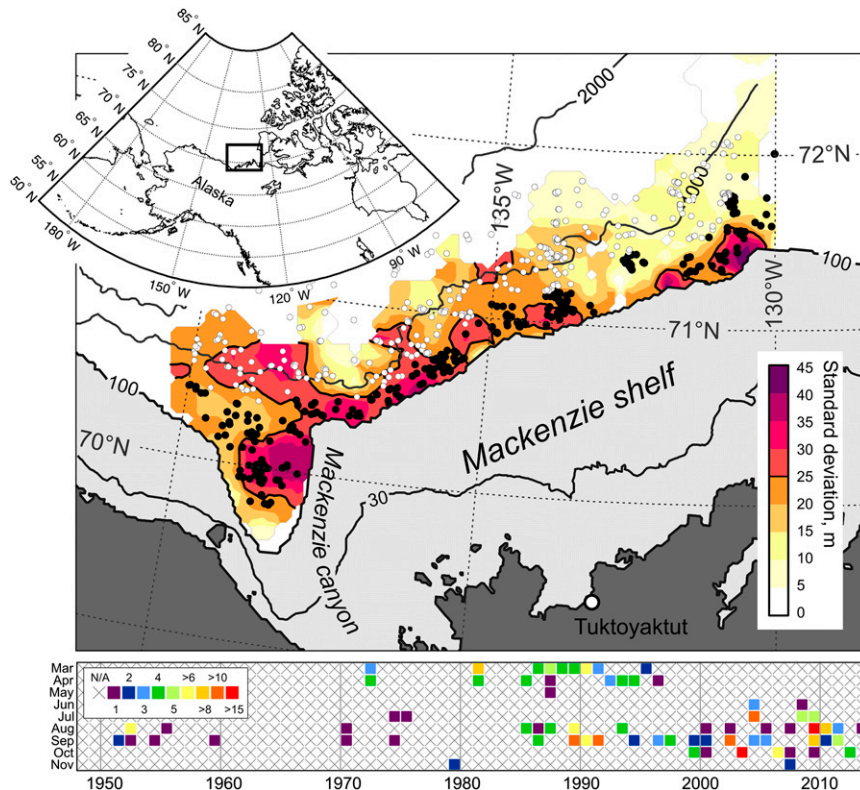


FIG. 1. (top) Map of the Mackenzie continental slope, including bathymetry (solid black line) and standard deviation of the -1.0°C isotherm depth (m). Black (white) dots indicate oceanographic stations taken between 100 and 600 m (600 and 2000 m) water depth contours where the -1°C isotherm and 33.4 isohaline were observed below 120-m depth. (bottom) The number of stations within 100–600 m isobaths between March and November in 1950–2013 are shown. The light gray shaded area in the top panel shows depths shallower than 100 m.

The long-term and seasonal changes of upwelling-favorable wind occurrence over the Mackenzie slope help us to demonstrate how the probability of upwelling events changes in time. The overall goal of the current study is to demonstrate the linkage between atmospheric wind forcing and changes in the offshore vertical thermohaline structure along the southern Beaufort Sea based on snapshot oceanographic measurements.

2. Data

This study is based on historical hydrographic (temperature and salinity) data collected in the second half of the twentieth century through to 2013. The data were kindly provided by the Arctic and Antarctic Research Institute (Russia) and include numerous archived CTD and bottle measurements carried out in the Beaufort Sea under different scientific programs. The number of stations in this dataset is roughly 2 times larger than available for this region via the World Ocean Database 2013. This dataset was used in several international

projects and in earlier studies (e.g., [Arctic Climatology Project 1997, 1998](#); [Dmitrenko et al. 2012](#); [Swift et al. 2005](#); [Polyakov et al. 2008](#)). For this research, we used a regional subset of oceanographic stations (i.e., those active over the Mackenzie continental slope) together with recent (2002–2013) observations made in the Beaufort Sea under the auspices of the Canadian ArcticNet project (www.arcticnet.org). The subset includes in situ measurements from various oceanographic platforms including aircraft and helicopter winter oceanographic surveys or ship-based summer oceanographic surveys. Most historical (prior to 1970s) temperature and/or salinity observations in this subset were made using Nansen bottles. In recent decades, measurements were made using conductivity–temperature–depth (CTD) instruments. All data were mandatorily quality controlled based on a standard 3σ tolerance test and additional subjective evaluations.

In the following, we use hydrographic profiles made between 140° and 130°W and water depth between 100 and 600 m, representing the Mackenzie slope region ([Fig. 1](#)). The total number of oceanographic profiles

gathered in this depth interval is 557, with 447 summer (July–October) and 102 winter (March–April) stations (Fig. 1, bottom). The deeper stations were not taken into account since the number of oceanographic stations dramatically decreases toward the deeper basin. In addition, we used 312 vertical profiles obtained between 600 and 1500 m just to demonstrate the general off-slope decrease of the -1°C isotherm depth variability (Fig. 1). We also found that upwelling effects are less pronounced north of the continental slope (results not shown).

In the following, we assume an accuracy of 10^{-2}C , typical for mercury reversing thermometers. Modern thermistors have an accuracy of 10^{-3}C or higher. The accuracy of titration for salinity samples in the historical dataset is 0.02 (Polyakov et al. 2008), while recent CTD salinity data and the Guildline Autosal technique have an accuracy of above 0.002. Note that the measuring technique for some historical records is not known. In these cases, we assume a lower bound accuracy of 10^{-2}C and 0.02.

The surface wind and sea level pressure (SLP) atmospheric data used in this study are from the National Centers for Environmental Prediction (NCEP) reanalysis. The wind speeds at 71°N , 135°W for both ice-free and ice-covered periods for the time period 1950–2013 were derived from the NCEP surface velocity data. The NCEP SLPs are in excellent agreement with 4- or 8-times-daily observations from Soviet drifting stations (from 1954 to 2006) through the entire Arctic, although a small systematic bias is present (Makshtas et al. 2007). Makshtas et al. (2007) also report a relatively high correlation (R^2 varied between 0.68 and 0.76 for different seasons) between the NCEP surface winds and observations, although the authors acknowledge that the errors in the wind observations at historical drifting camps are high. For the area considered in this study, Williams et al. (2006) reported “some confidence to the NCEP winds” based on comparison of NCEP data over the Mackenzie continental shelf with wind speed observed at coastal meteorological stations.

3. Methodology

To quantify upwelling, Carmack and Kulikov (1998) introduced the so-called effective depth (ED). The ED was defined as the level where the reference vertical salinity profile—representing a typical water-mass structure at some location off slope—is equal to the CTD-observed salinity near the bottom of the shelf. Williams et al. (2006) suggested that the reference temperature profile can also be used to calculate the ED over the Mackenzie slope within the layer of monotonically increasing temperature between 180 and about 500 m. But authors noted that a small variation of temperature and

salinity at every depth among the off-slope CTD casts taken at the reference location is required for reliable ED estimations. From a climatological perspective, the decadal variability in temperature and salinity makes this method difficult since it suggests a known reference temperature–salinity (TS) profile for every oceanographic station taken over the continental slope throughout all historical records.

To avoid these difficulties, we correlate instead the surface wind (the independent variable) and the depths of a given isotherm/isohaline in the vertical TS profiles (dependent variables), which are not predetermined but can be specified depending on the local vertical thermohaline structure. One of the eligible criteria for choosing a given isotherm or isohaline could be its vicinity to the depth of maximum temperature or salinity variations in TS profiles that can be associated with vertical displacement resulting from episodic upwelling and downwelling events. As a special case for mooring records, Spall et al. (2008) and Pickart et al. (2009) used the mean monthly near-bottom salinity to identify upwelling events. For the Alaskan shelf, Tsimitri and Pickart (2006) suggested using the -0.8°C isotherm and 33.8 isohaline as a pair of parameters that can be used to identify the presence of Atlantic Water, uplifted during upwelling. Although Carmack and Kulikov (1998), Williams et al. (2006), and Pickart et al. (2009) argue that salinity is the preferred indicator characterizing upwelling on the Beaufort Sea shelf, temperature can also be used as a criterion to identify upwelling of warmer Atlantic Water for the depth interval where temperature monotonically increases with depth. For the Mackenzie slope, we arbitrarily choose the -1°C isotherm (instead of -0.8°C) because of its correspondence with the 33.8 isohaline, another parameter describing AW inventory (Tsimitri and Pickart 2006; see below for details). Although the wind-driven upwelling is not the only source of observed changeability of the -1°C isotherm and 33.8 isohaline positions determined from snapshot measurements, we find that correlation analysis provides an effective way to constrain the effect of other processes on water displacements over the steep topography. Processes that can affect isohaline and/or isotherm positions include the coastally trapped waves propagating along the continental slope, the changes of stratification associated with long- and short-term thermohaline changes in the Beaufort Sea, and the eddies and meanders. However, the water displacements associated with these processes seem to be randomly distributed in time and space and are not related to the local cumulative wind forcing.

Although the air–ocean or ice–ocean surface stresses are more directly related to the energy transferred to the

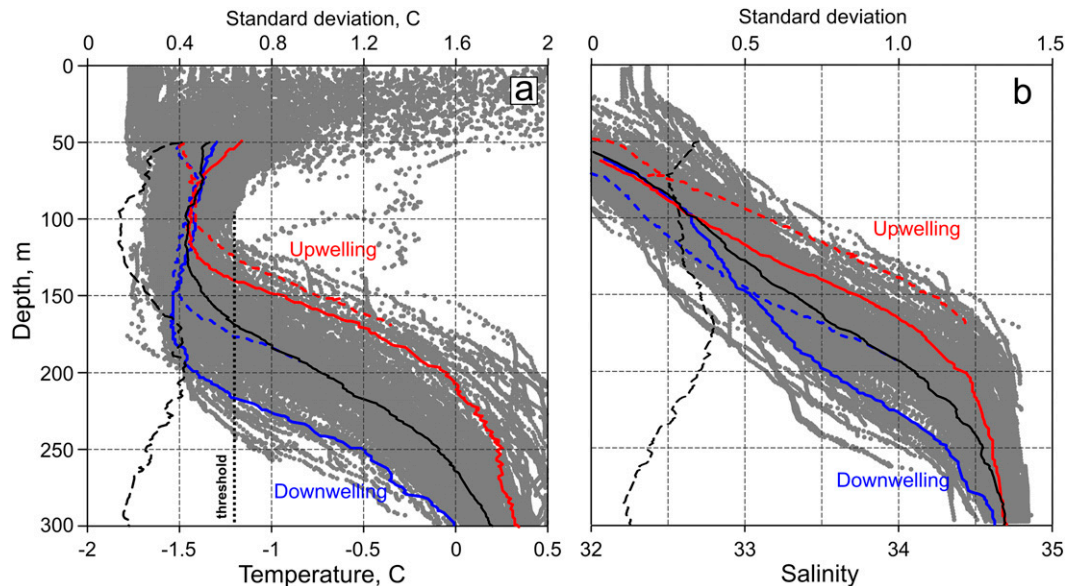


FIG. 2. Scatterplot of (a) temperature ($^{\circ}\text{C}$) and (b) salinity for all hydrographic stations from 1950 to 2013. The solid and dashed black lines below 50 m depict mean profiles and their standard deviations, respectively. Red and blue lines indicate the average profiles corresponding to the presumable extreme ($D_{-1^{\circ}}$ and $D_{33.8}$ are beyond plus or minus one standard deviation) upwelling and downwelling events observed for 200–600 (solid lines) and 100–200 m (dashed lines). Dotted threshold line indicates -1.2°C below 100 m (see explanation in the text).

surface layer, we use the wind speed instead because of the difficulties in estimating ice–ocean surface stresses in ice-covered regions. Since winds steadily blowing in the same direction for a long time have a greater impact on upwelling dynamics (e.g., Bakun 1973; Carmack and Kulikov 1998; García-Reyes et al. 2014), we present results for 1–80-day average winds prior to the reported date of each oceanographic station.

4. Results

The Atlantic Water on the Mackenzie continental slope are identified by a temperature increase at intermediate water depth of 120–200 m (Fig. 2a). The maximum temperature and salinity variances are observed at approximately 200- and 170-m depths, respectively (Fig. 2). We interpret this high variance in temperature and salinity as vertical displacement of the AW upper boundary, although decadal variations of the AW thermal state and/or freshwater content in the surface layer can also affect the boundary position (Zhong and Zhao 2014). The average depth of the -1.0°C isotherm over the Mackenzie slope is 185 m, in reasonable agreement with the mean depth of 33.8 isohaline (181 m). The spatial pattern of the -1.0°C isotherm depth standard deviations interpolated on a $10 \times 10 \text{ km}^2$ grid show higher variability along the Mackenzie slope while the variability decreases off slope (Fig. 1).

Note that the average distance between stations is approximately 6–8 km. This results in approximately 10–20 stations within a 15-km search radius, making the pattern shown in Fig. 1 rather robust.

With few exceptions the temperatures exceeding the -1.2°C threshold value monotonically increase from approximately 120 (Fig. 2a) to approximately 400–500 m, where the local maximum of long-term mean temperature of $+0.41^{\circ}\text{C}$ associated with the AW core is observed (not shown). Considering the steady salinity increase with depth, it implies that the -1.0°C isotherm and 33.8 isohaline can be used to identify vertical displacement associated with wind-forced upwelling over the Mackenzie continental slope. Moreover, the mean -1°C isotherm and 33.8 isohaline depths (hereinafter referred as $D_{-1^{\circ}}$ and $D_{33.8}$, respectively) approximate those of maximum temperature and salinity variances, suggesting that $D_{-1^{\circ}}$ and $D_{33.8}$ are reliable predictors indicating vertical displacement associated with upwelling or downwelling events (Fig. 2). Although the total amount of oceanographic stations and their temporal coverage are different for different ocean depth ranges, the increase in mean $D_{-1^{\circ}}$ and $D_{33.8}$ are statistically significant at around the 200-m isobath (Fig. 3b), whereas mean $D_{-1^{\circ}}$ and $D_{33.8}$ are relatively stable at 200–600-m bottom depths (hereafter referred to as the deep zone, in contrast with the shallow 100–200-m zone of continental slope). Large interannual

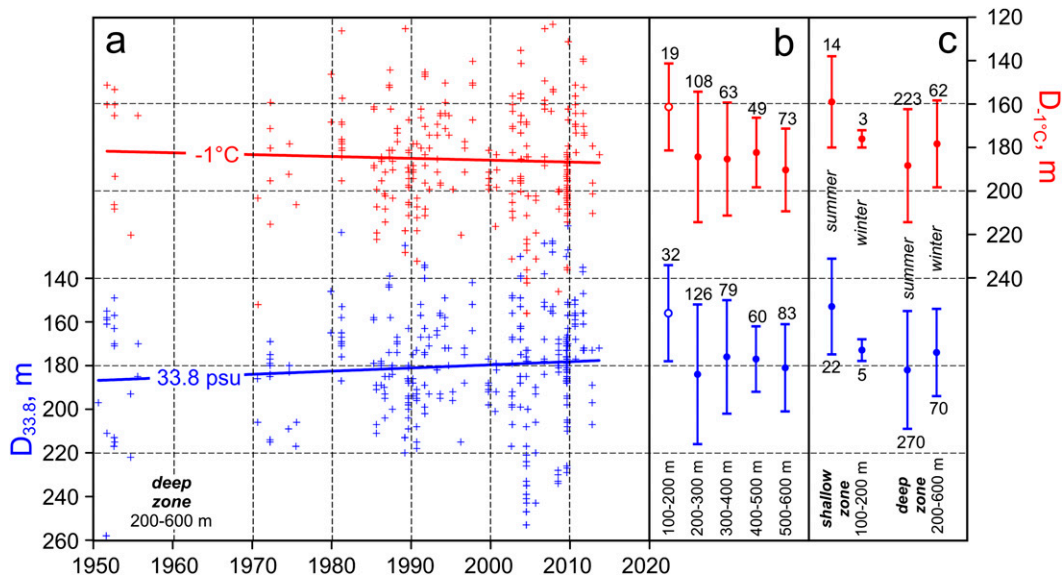


FIG. 3. (a) Depths (m) of the -1°C isotherm and 33.8 isohaline (red and blue crosses, respectively) for 200–600-m water depths and linear trends. Mean depths and standard deviations for different (b) depth ranges and (c) seasons. The numbers above the standard deviation bars indicate the total number of stations in the different depth zones and seasons.

variability is present in both $D_{-1^{\circ}}$ and $D_{33.8}$, with statistically nonsignificant linear trends of 0.9 and $-1.4\text{ m decade}^{-1}$, respectively (Fig. 3a). The high correlation between $D_{-1^{\circ}}$ and $D_{33.8}$ of $+0.96$ indicates the synchronous vertical displacement of isotherms and isohalines.

To account for the cumulative effect of wind forcing we calculate the linear correlations between $D_{-1^{\circ}}$ or $D_{33.8}$ in the deep zone and the preceding wind speed averaged over different averaging intervals (ranging from 1 to 80 days) and projected at different directions (0° – 360°). The correlation analysis allows us to identify the temporal scale and direction of wind forcing resulting in the most prominent isotherm and isohaline displacements but not to quantify this impact. Therefore, this approach demonstrates only the most probable direction of upwelling- or downwelling-favorable winds and their temporal scale. The highest correlations and corresponding wind directions are plotted in Fig. 4 for each averaging time period. To take into account the effect of sea ice on upwelling event, the correlations are presented separately for (i) summer (July–October), when free drift conditions are commonly observed over the Mackenzie continental slope, and (ii) winter (March–April), when a consolidated sea ice cover dominates (Carmack and Macdonald 2002; Barber and Hanesiak 2004; Williams and Carmack 2015). In the shallow (100–200 m) zone, only the correlations between wind and $D_{33.8}$ measured in summer were obtained as a

result of the insufficient data coverage (Fig. 4a) during the winter.

Statistically significant (at the 95% confidence level) correlations between $D_{-1^{\circ}}$ or $D_{33.8}$ and northeast (NE) winds are present for both seasons, although the wind directions from north-northeast to east-northeast can also be considered effective (Fig. 4b). The negative values indicate the ascent of isotherms/isohalines for the NE winds, whereas the southwest (SW) winds cause a descent in isotherms/isohalines. The maximum correlations during the summer ice-free periods are significantly higher than during winter, although winter correlations exceed those for summer for averaging periods longer than 27 days (Fig. 4a). In the deep zone, there is a correlation of between -0.52 and -0.58 for an approximate 20-day cumulative wind forcing (corresponding to 27%–34% of the total variance of $D_{-1^{\circ}}$ or $D_{33.8}$ explained by wind impact). In the shallow zone there is a maximum correlation of -0.74 (55% of total variance) for a cumulative wind forcing of 19–21 days (Fig. 4a). In winter, correlations gradually increase with longer cumulative wind forcing; the maximum values of -0.38 and -0.47 for $D_{-1^{\circ}}$ and $D_{33.8}$, respectively (14% and 22% of total variance) are found for cumulative wind forcing of 48 days and then correlations decrease for longer time scales (Fig. 4a).

The maximum correlations are associated with a relatively long cumulative wind forcing for both seasons, although the response of isohaline and isotherm depths to the NE winds is also clear for shorter wind averaging

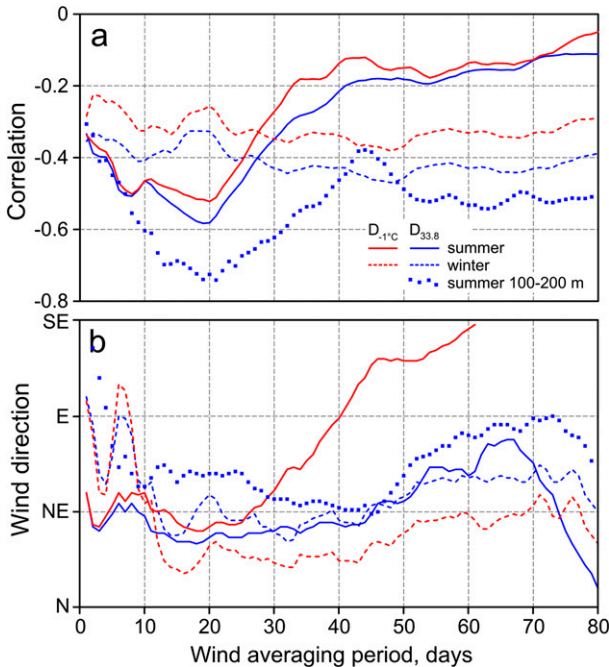


FIG. 4. (a) Maximum correlations between the mean NCEP wind velocities at 71°N , 135°W (averaging period is on the x axis) and D_{-1° (red lines) and $D_{33.8}$ (blue lines) for the 200–600-m zone and (b) the wind directions associated with the maximum correlation shown in (a). Solid and dashed lines indicate summer (July–October) and winter (March–April), respectively. Blue squares show maximum summer correlations for the shallow 100–200-m zone.

periods. For instance, the correlations of D_{-1° and $D_{33.8}$ with instantaneous wind (corresponding to 1-day averaging period) are approximately -0.30 and -0.35 . For an averaging period of 8 days—a typical time scale for storms on the Alaskan coast (Pickart et al. 2013b)—the summer correlations exceed -0.50 for both D_{-1° and $D_{33.8}$ and the correlations in winter are -0.31 and -0.39 , respectively (Fig. 4a). Hereafter we use an averaging period of 8 days, following Pickart et al. (2013b), as a time interval that is sufficient for the development of upwelling or downwelling along the Mackenzie slope. For simplification, we continue using the term “NE” for the upwelling-favorable wind direction, but the wind projection at 239° ($T59^\circ$) was intrinsically used as a mean direction found for 8-day averaging periods (Fig. 4b).

To characterize the typical large-scale atmospheric patterns that result in upwelling or downwelling at the Mackenzie slope, we construct a composite of SLP over the Canadian Arctic for periods when D_{-1° and $D_{33.8}$ within the deep zone of the Mackenzie slope exceed the mean by plus or minus one standard deviation—that is, for conditions when extreme upwelling and downwelling events are presumably present

(see Fig. 2). The mean upwelling- and downwelling-favorable 8-day-averaged SLPs corresponding to these displacements are shown in Fig. 5. During both summer and winter, the upwelling, characterized by shallower isotherms and isohalines, is evident when easterly geostrophic winds over the Mackenzie slope are present. These winds are closely related to the presence of two climatological centers of action—the Beaufort high (BH) in the Canadian basin and the Aleutian low (AL). Both the BH and AL are located at approximately the same positions during extreme upwelling events in summer and winter, although both centers are weaker during the ice-free season (Figs. 5a,d). Despite the smaller SLP difference between BH and AL in summer (15.2 vs 24.1 hPa during winter) the cross-slope SLP gradients over the Mackenzie shelf are higher, suggesting the presence of stronger easterly winds during extreme upwellings. In winter, the zone of high SLP gradients is shifted southward toward the center of Alaska, leading to weaker easterly winds over the Mackenzie shelf when compared to July–September.

The downwelling cases in summer are also controlled by two centers of action in the atmosphere: a low pressure system located in the central part of the Canadian basin and a high pressure center in the North Pacific. Both centers are weak when compared with upwelling-favorable situations, and the lateral gradient of SLP is weak in the southern Beaufort Sea (Fig. 5b). In winter, extreme downwelling events are associated with the BH shifted toward the Alaskan coast leading to westerly winds over the Mackenzie shelf (Fig. 5e). However the small number of winter hydrographic data strongly limits our confidence in the derived SLP patterns for extreme downwelling and upwelling cases in March–April.

To quantify the impact of the AL and BH on the vertical displacement of isohaline and isotherm over the Mackenzie slope we calculate the correlations between the 8-day-averaged SLP and D_{-1° for summer (Fig. 5c) and winter (Fig. 5f). These patterns clearly indicate a dipole mode of SLP with negative correlations over the Canadian basin corresponding to an uplift of isotherms when atmospheric pressure increases and positive correlations over the North Pacific implying the opposite effect of atmospheric pressure on the depth of isotherms. Although the locations of dipole extrema (maximum and minimum correlations) do not coincide with the 1948–2014 mean seasonal position of the AL and BH centers (shown with black crosses), the mismatch can be attributed to the wide variety of different synoptic types of atmospheric forcing (Asplin et al. 2009) having a similar effect on the cross-shelf Ekman transport and, hence, upwelling or downwelling over the Mackenzie slope.

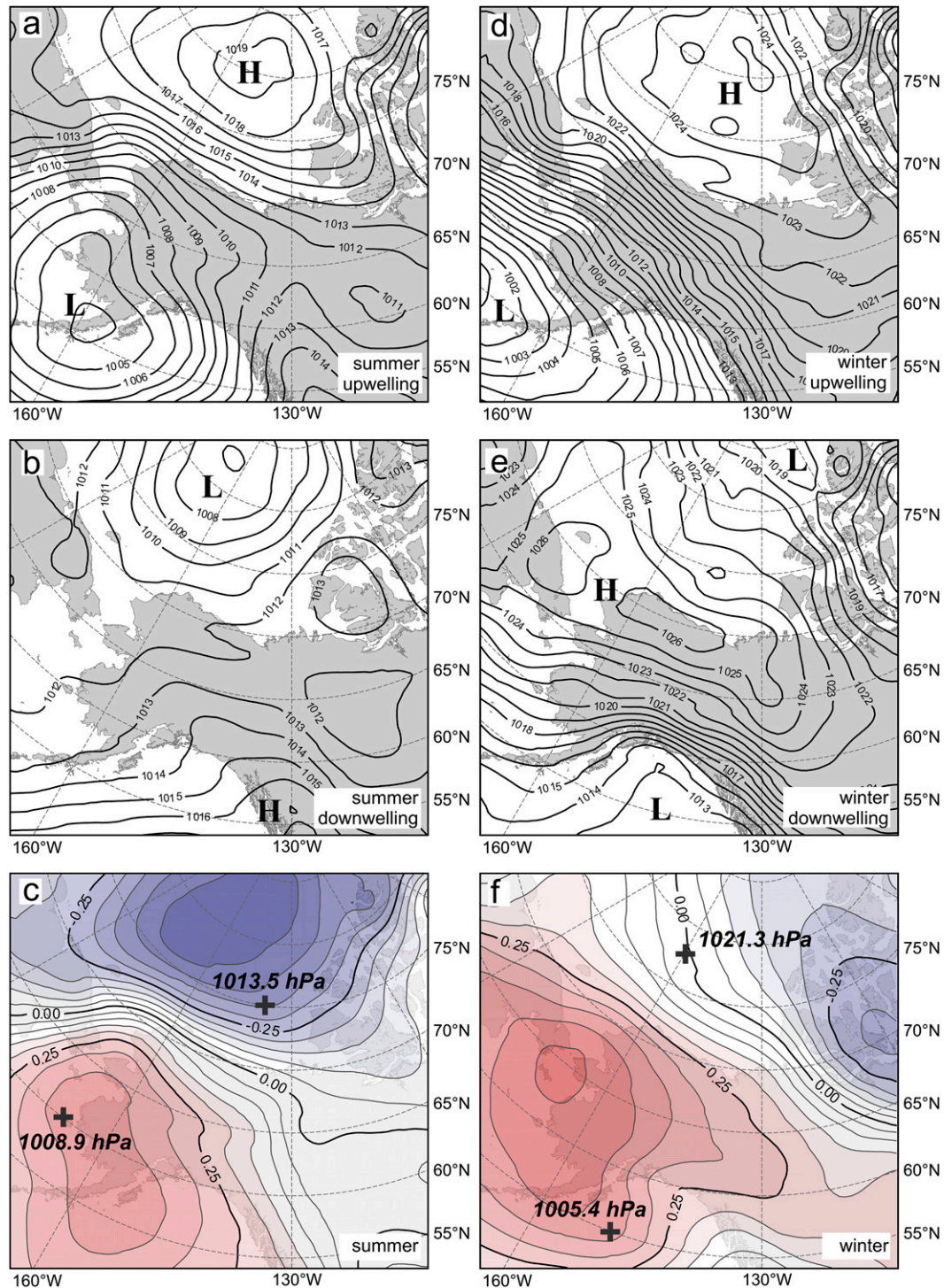


FIG. 5. The mean (a),(b) summer and (d),(e) winter sea level pressure (hPa) for all years with (a),(d) upwelling and (b),(e) downwelling isotherms and isohalines exceeding plus or minus one standard deviation from mean D_{-1} and $D_{33.8}$ within the deep zone of the Mackenzie slope. Black crosses and numbers indicate the 1948–2014 mean Aleutian low and Beaufort high positions and central SLPs for (c) July–October and (f) March–April. The linear correlations between D_{-1} and SLP for an 8-day averaging period preceding the event are shown for summer in (c) and winter in (f).

5. Discussion

The CTD profiles and water samples collected over the Mackenzie continental slope show considerable variability in temperatures and salinities for water depths ranging between 170 and 220 m (Fig. 2). This variability seems to be associated with the vertical water displacements caused by wind-forced upwelling and downwelling. The standard deviations of D_{-1° and $D_{33.8}$, which roughly indicate the position of the AW upper boundary, are 22–27 m during summer and approximately 20 m during winter. These deviations are an order of magnitude lower than the maximum values of isopycnal displacement (up to ~400 m) estimated from the near-bottom salinity observations at moorings in the Mackenzie Trough in 1987/88 (Carmack and Kulikov 1998; Williams et al. 2006) and over the Mackenzie continental slope in 2009–11 (Jackson et al. 2015). However, the standard deviations of ED estimated from mooring records in 2009–11 (moorings B and H; see Jackson et al. 2015) vary from 29 to 62 m (J. Jackson 2015, personal communication). These quantities are considerably closer to our standard deviations of 20–27 m estimated from snapshots of vertical temperature and salinity profiles. The remaining difference can be partly attributed to the unresolved bottommost portion of the water column during oceanographic surveys over the continental slope, whereas the largest vertical displacements occur within the tens of meters above the bottom during upwellings and downwellings (see, e.g., Pickart et al. 2013b, their Fig. 17c). Another reason is the limited data collection during strong wind events; the shipborne operations are limited during severe storms when the intense upwelling events are present.

A statistical analysis of observed reference depths for the -1°C isotherm and 33 isohaline was conducted in order to determine upwelling-favorable winds and consider their cumulative effect on the water column. The statistically significant (at the 95% confidence level) correlations with along-slope northeasterly winds ($T59^\circ$) were found for the time series of D_{-1° and $D_{33.8}$ over the deep (200–600 m) zone during both summer and winter. The correlations generally increase with the length of the averaging period for the wind speed in agreement with results of Carmack and Chapman (2003), who suggested a typical time of upwelling stabilization of 3 days under ice-free conditions based on numerical modeling. The northeasterly winds cause off-slope Ekman transport in the surface layer, which induces divergence and upwelling of deep waters toward the Mackenzie shelf. The higher correlations for longer averaging periods indicate a stronger effect of the cumulative wind forcing on the cross-slope Ekman transport, which continues as long as wind stress is applied (Carmack and Chapman 2003).

During the ice-free period, the maximum correlations (and, hence, the wind-induced vertical displacement) from -0.52 to -0.58 are found for the 20-day averaging period for NE winds (Fig. 4a). This implies that, although the variance of the 20-day mean wind speed is much lower than that for the daily winds (2.2 vs $20.3\text{ m}^2\text{ s}^{-2}$), weak but persistent winds blowing in the same direction result in a stronger cumulative effect of water exchange between the basin and shelf (both upwelling and downwelling). In the shallow 100–200-m zone, the same averaging period for the wind results in an even higher significant correlation of -0.74 , although the data scarcity (only 22 stations) has to be noted. The more pronounced wind impact in the shallow zone can be attributed to the closer position of -1°C isotherms and 33.8 isohalines to the sea floor where the largest amplitudes of water displacement are observed during the upwelling episodes (e.g., Estrade et al. 2008; Pickart et al. 2013b).

In winter, the presence of consolidated pack ice substantially modifies the surface Ekman transport over the Mackenzie shelf and causes the asymmetry in the ice–ocean stresses for different wind directions (Williams et al. 2006). For instance, persistent easterly winds induce offshore ice transport over the Mackenzie shelf, resulting in the development of numerous leads, a decrease in ice concentration, and, hence, an increase in ice–ocean momentum transfer (Martin et al. 2014). Conversely, westerly winds lead to onshore ice transport, a consolidation of the pack, and a reduction in the ice–ocean momentum transfer (Williams et al. 2006). Although winds that are favorable for upwelling events during winter should cause the largest amplitude of upwellings (Carmack and Kulikov 1998; Jackson et al. 2015), the asymmetry between easterly and westerly winds results in generally lower maximum correlations between the wind and D_{-1° and $D_{33.8}$ (-0.38 and -0.47 , respectively; Fig. 4a) when compared to the ice-free season. However, sea ice does not considerably change the fact that longer wind impact results in a larger upwelling event; the maximum negative correlations in winter are found for NE winds blowing for 1–2 months or more (Fig. 4a), but the correlations are still statistically significant for the synoptic-scale forcing of 8–10 days for both summer and winter.

The relatively small part of total D_{-1° and $D_{33.8}$ variance associated with the wind forcing (varied from 14% to 55%) indicates that other oceanographic processes considerably affect the changeability of isotherm and isohaline depths over the Mackenzie slope. However, the applied correlation method has certain disadvantages that are related to the complexity of wind impact on upwelling or downwelling events. For instance, the same isohaline and isotherm displacements can be

formed under two different scenarios: the relatively short but strong wind event and the long-lasting but weak wind. This effect might result in a lower level of similarity between the time series of D_{-1° or $D_{33.8}$ and averaged wind that leads to underestimation of wind-driven signal in isotherm and isohaline displacements.

We calculated the mean SLP patterns associated with extreme upwelling and downwelling episodes along the Mackenzie slope during summer and winter. The key factor affecting the effectiveness of upwelling events associated with easterly winds is the difference in SLP between the cores of BH and AL. During extreme upwelling events, this difference is 15.2 and 24.1 hPa for summer and winter, respectively (Figs. 5a,d), with a climatological (1948–2014) mean difference in SLP between BH and AL centers of approximately 4.6 and 15.7 hPa (Figs. 5c,f). This implies that upwelling-favorable wind conditions are observed when the AL is deeper ($-5.0/-4.5$ hPa in summer/winter) and the BH is anomalously high ($+5.6/+3.7$ hPa in summer/winter) compared to the mean state. The summer and winter atmospheric forcing shown in Figs. 5a and 5d resemble those reported in Pickart et al. (2013a) as upwelling-favorable winds along the Alaskan Beaufort Sea continental slope in August and May. We conclude that upwelling over the entire southern Beaufort Sea continental margin including the Mackenzie slope is driven by identical large-scale atmospheric processes characterized by the relative strength of the Aleutian low and Beaufort high.

Downwelling-favorable winds in winter are also associated with a strong BH that is considerably shifted south toward the Alaskan coast (Fig. 5e). Under these conditions, the anticyclonic atmospheric circulation around BH results in westerly geostrophic winds over the Mackenzie shelf. In this case, the downwelled waters at intermediate depths compensate the onshore Ekman transport in the surface layer. In contrast to winter, downwelling favorable situations in summer are associated with a low pressure system located over the Canadian basin (Fig. 5b). Both winter and summer downwelling can be attributed to periods of Beaufort Gyre reversals when the ice motion in the Beaufort Sea is switching from an anticyclonic to cyclonic regime coinciding with reversals of the large-scale atmospheric circulation over the Canadian basin (Lukovich and Barber 2006; Asplin et al. 2009). For instance, extreme winter and summer downwelling events occur when the atmospheric circulation pattern resembles the cyclonic types 6 and 1, respectively, according to the classification of Asplin et al. (2009). These types are generally characterized by decrease of SLP from the Mackenzie shelf toward the central Canada Basin. The frequency of

occurrence of cyclonic type 6 between November and April is 9.3%, while the frequency of occurrence of cyclonic type 1 is 24.6% from May to October. Altogether the occurrence of a cyclonic circulation pattern over the Beaufort Sea (types 1, 6, and 7) are 21.9% and 37.4% in November–April and May–October, respectively (Asplin et al. 2009, their Table 2). This is indicative of more frequent Beaufort Gyre reversals during summer compared to winter (Asplin et al. 2009). Considering that the circulation in the Canada Basin is anticyclonic on average and the fact that reversals are relatively short lived, downwelling events can be thought of as a relaxation of generally uplifted isotherms and isohalines over the Mackenzie continental slope. More precisely, the relaxation occurs when persistent northeasterly winds associated with frequent low pressure cyclones and storm activities (Hudak and Young 2002; Asplin et al. 2009) are weakened or reversed.

From a physical and biological point of view, upwelling events are a substantial mechanism increasing cross-shelf exchanges and supplying deep nutrient-enriched waters to the surface layer over the Mackenzie continental slope. In the following we link extreme upwelling events to known large-scale climate indices and/or SLP difference between the Beaufort high and the Aleutian low. The sparsity of oceanographic measurements does not allow for a clear characterization of the long-term evolution of upwelling occurrence over the Mackenzie slope. Instead, we use NCEP northeasterly wind as a proxy for upwelling-favorable conditions, following the approach of Pickart et al. (2013a), who reported a good correlation between long-term trends in along-slope wind speed and the probabilities of upwelling events at Point Barrow, Alaska.

We observe a clear decadal signal in the mean seasonal upwelling-favorable 8-day-averaged NE winds (Fig. 6a). The long-term means of the NE winds are 0.96 and 0.83 m s^{-1} for summer and winter, respectively. Positive values indicate a dominant anticyclonic circulation regime over the Beaufort Sea, although negative values (corresponding to the southwesterly winds and cyclonic type of atmospheric circulation) are often observed in 1954–64, 1970–75, and 1985–97 (Fig. 6a). The increase in the mean NE winds for both summer and winter begins at the end of the 1990s, with a dramatic increase in the summers of 2007, 2010, and 2011, presumably associated with an amplified summer Beaufort Sea high (Moore 2012; Wood et al. 2013; Williams and Carmack 2015).

The probability of occurrence of extreme NE wind was estimated based on the length of time when the northeasterly wind speed exceeded the long-term seasonal mean plus one standard deviation (of 2.80 and

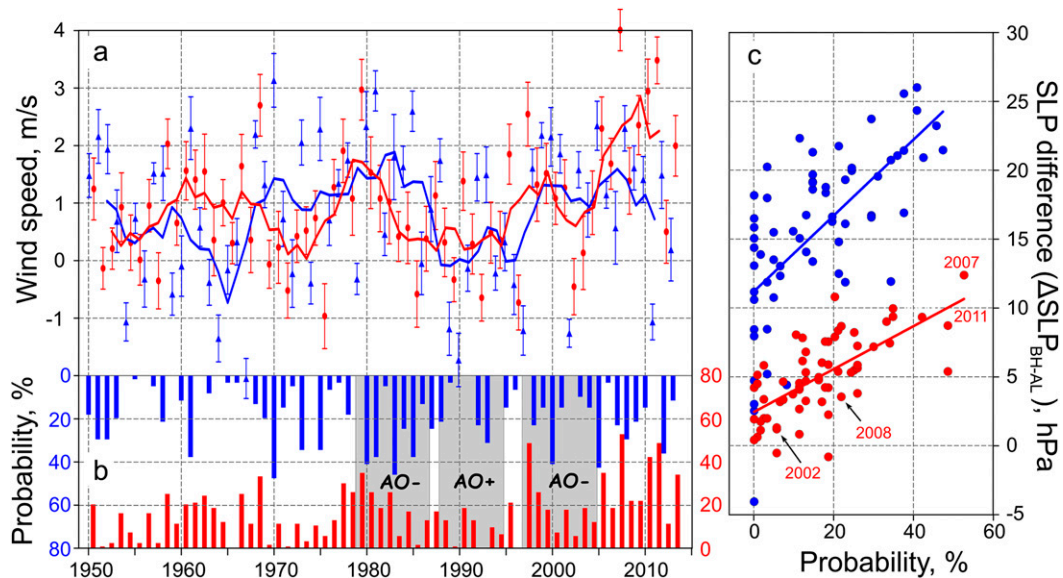


FIG. 6. (a) Seasonally averaged winter (blue triangles) and summer (red dots) 8-day northeast ($T59^\circ$) wind speed at 71°N , 135°W . Vertical error bars show the standard deviation for each season (divided by 5). The red and blue lines are the 5-yr running mean for summer and winter, respectively. (b) Probability of upwelling-favorable wind speeds exceeding the long-term seasonal mean plus one standard deviation for the winter (blue; left y axis) and summer (red; right y axis). (c) Scatterplot of the probability of upwelling-favorable wind events and SLP difference between the BH and AL for the summer (red) and winter (blue) for different years. The linear best fit is shown as a blue line for winter and red line for summer.

2.59 m s^{-1} for summer and winter, respectively). The high correlation between the probability of occurrence and the mean seasonal NE wind speed ($+0.91$ and $+0.81$ for summer and winter, respectively) is in agreement with results by Pickart et al. (2013a) and confirms the relationship between high probability of upwelling events and more intensive anticyclonic circulation (Fig. 6b). To relate the observed interannual to decadal variability in upwelling with large-scale atmospheric circulation patterns, we examine the seasonal means of known atmospheric indices including the Arctic Oscillation (AO; Thompson and Wallace 1998) and North Pacific index (NPI; Trenberth and Hurrell 1994). Both indices describe different aspects of the large-scale atmospheric circulation patterns over the Arctic and North Pacific, which can further affect the local atmospheric processes in the Beaufort Sea. The AO is related to the dominant mode of vorticity over the Arctic domain (cyclonic vs anticyclonic), which is linked with the strength of the Beaufort high and strength of the anticyclonic circulation (Polyakov and Johnson 2000; Rigor et al. 2002). On the other hand, the NPI represents the area-weighted SLP over the Bering Sea and North Pacific and reflects the strength of the Aleutian low (Rodionov et al. 2005). When combined together, the AO and NPI can be used as a proxy for changes in the regional storm tracks and wind regime over the southern Beaufort Sea and, hence,

changing of upwelling or downwelling water displacements over the slope.

We found no statistically significant correlation between the NPI and the occurrence of upwelling during summer. However, small but statistically significant correlations (-0.30) were found between the AO and occurrence of upwelling for both summer and winter. A weak correlation between extreme upwelling and the AO index was also reported by Yang (2009), who investigated Ekman pumping and the associated long-term upwelling/downwelling vertical water velocities in the Beaufort Sea from 1979 to 2006. Yang (2009) demonstrated that upwelling over the Alaskan and Canadian coast was intensified when the AO was in its negative phase (in 1979–86 and 1997–2004), while periods of relatively high AO index (1988–94) correspond to weaker upwelling, although no significant correlation over the 28-yr period was found (Yang 2009). This is in agreement with results shown in Fig. 6b showing generally lower mean probabilities (9% and 11%) of extreme upwelling-favorable winds during the 1988–94 time period for summers and winters, respectively. In contrast, the mean summer and winter probabilities during low AO (19% and 20%, respectively) are about 2 times higher. The highest (statistically significant) correlation (-0.52) was found between the winter upwelling occurrence and the NPI. This correlation implies

that the decreasing of SLP in the Aleutian low during the negative NPI phase results in an intensification of northeasterly winds over the Mackenzie slope and increased off-slope Ekman transport. This result is in contrast to [Pickart et al. \(2013a\)](#), who reported no significant correlations between NPI and number of upwelling events associated with easterly winds exceeding 10 m s^{-1} for at least four days for the Alaskan slope.

Considering the results shown in [Figs. 5c,f](#) and the reasonably high correlations of upwelling-favorable winds with large-scale atmospheric indices, one can expect that the magnitude of the SLP difference between the Aleutian low and Beaufort high greatly affects the intensity of upwellings over the Mackenzie sea slope. To estimate the role of each center of action, we correlated the probabilities of upwelling-favorable winds over the Mackenzie shelf with SLP in the mean climatological (1948–2014) centers of AL and BH (shown with black crosses in [Figs. 5c and 5f](#) for summer and winter, respectively). Both centers have a comparable impact on the upwelling probabilities, although the correlations with the BH SLP are higher than those with AL ($+0.56/+0.53$ vs $-0.46/-0.41$ during summer/winter). This result is in line with that reported by [Brugler et al. \(2014\)](#), who demonstrated the larger effect of BH intensification on the easterly winds in the Alaskan Beaufort Sea compared to the Aleutian low deepening. The combined effect of both centers can be expressed as the differences between the seasonal mean SLPs in the BH and AL ($\Delta\text{SLP}_{\text{BH-AL}}$). The resulting correlations between $\Delta\text{SLP}_{\text{BH-AL}}$ and extreme wind probabilities are $+0.68$ and $+0.66$ for summer and winter ([Fig. 6c](#)), confirming that both BH and AL are of importance and contribute to the intensity of the upwelling-favorable winds. However, the relative position and configuration of both centers can also play a significant role ([Pickart et al. 2013a](#)) resulting in a wide range of upwelling-favorable wind probabilities for the same SLP differences between BH and AL ([Fig. 6c](#)). Moreover, there is well-pronounced seasonality in upwelling-favorable wind probabilities that strongly correlates with the seasonal cycle of NE wind speed over the Mackenzie slope ([Fig. 7](#)). The individual correlations between the upwelling probabilities and $\Delta\text{SLP}_{\text{BH-AL}}$ during winter and summer seasons estimated for half-month spans varied between $+0.47$ and $+0.74$ ([Fig. 7](#)). These estimates are modest compared to $+0.68$ and $+0.66$ values found based on smoother mean seasonal time series of probabilities and $\Delta\text{SLP}_{\text{BH-AL}}$. Although we found no pronounced seasonal cycle in the individual correlations, one can suggest that stronger winds blowing in April–June and September–October may considerably increase the

probability of upwelling events over the Mackenzie slope regardless of the actual SLP difference between the Beaufort high and Aleutian low.

While the seasonal mean $\Delta\text{SLP}_{\text{BH-AL}}$ can be used to identify probabilities of upwelling event occurrence over the Mackenzie slope, it cannot be used to predict individual upwelling episodes. For instance, the upwelled cold, salty, and nutrient-rich waters that were found at the Mackenzie shelf in 2002 ([Garneau et al. 2006](#)), 2007 and 2008 ([Tremblay et al. 2011](#); [Gratton et al. 2012](#)), and 2011 ([Mathis et al. 2012](#)) all occurred in summers when the occurrence probabilities varied in a wide range from 6% (in 2002) to 53% (in 2007; [Fig. 6c](#)).

6. Conclusions

We have presented an analysis of seasonal patterns and interannual evolution of upwelling events over the Mackenzie continental slope based on individual historical hydrographic observations. The variability in temperature and salinity at intermediate depths over the Mackenzie slope, associated with vertical displacement of the upper boundary of Atlantic Water, is large and is correlated significantly with along-slope winds. The effect of wind forcing is more pronounced under ice-free conditions, and the correlation between along-slope winds and upwelling at the shelf break is highest when wind is integrated over a period of 20 days before a given upwelling event. In winter, the largest effect is associated with winds steadily blowing along the slope for a period of 1–2 months, although the linkage between the NE wind and isohaline or isotherm displacement is still reasonably high at the synoptic periods of 8–10 days both in summer and winter. The location and central pressure of the Beaufort high and Aleutian low largely control occurrences of upwelling- or downwelling-favorable wind patterns. The summertime amplification of the BH is responsible for the predominant upwelling-favorable conditions over the Mackenzie slope in recent decades. The probability of upwelling-favorable wind occurrence is closely linked to the sea level pressure difference between the BH and AL, although the locations of both pressure centers also strongly affects the wind pattern. In turn, the seasonality of wind forcing produces higher probability of upwelling occurrences in April–June and August–October—periods when the mean climatic NE wind speed exceeds 1 m s^{-1} .

These results are of interest in the context of the recent warming in the Arctic. Reduction in sea ice extent and thickness and the lengthening of the ice-free season may cause longer periods with enhanced cross-slope exchange through upwellings and downwellings as suggested by [Carmack and Chapman \(2003\)](#). Atmospheric pressure

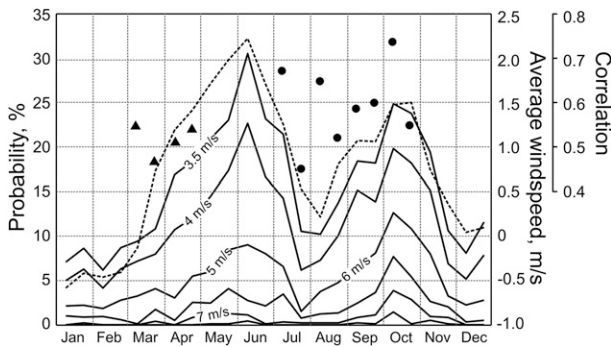


FIG. 7. The half-monthly averaged NE ($T59^\circ$) wind speed evaluated from 1948–2013 NCEP data at 71°N , 135°W (dashed line). Black solid lines correspond to the mean climatic probabilities of 8-day-averaged NE wind speeds exceeding a certain threshold level (3.5 m s^{-1} , 4 m s^{-1} , ...)—that is, the upwelling-favorable conditions, also shown for half-month spans. Black symbols indicate the correlation between probabilities of upwelling-favorable NE ($T59^\circ$) wind speeds exceeding 3.5 m s^{-1} and SLP difference between the BH and AL in their mean summer (triangles) and winter (dots) positions.

patterns dominate surface wind forcing of oceanic upwelling and downwelling, and the analysis here provides ample evidence of the strength of this coupling in time. We also recognize that at the regional scale feedbacks between the surface and atmosphere can also affect the strength and position of both low and high pressure patterns and that climatological changes in sea ice have the potential of feeding back into how local surface winds affect dynamics of ocean–sea ice–atmosphere interface (e.g., Asplin et al. 2015), relative to the fixed geography of shelf–basin geometry. Moreover, the decrease of sea ice thickness and extent would result in higher sea ice drift velocities (Yang 2009; Spreen et al. 2011) providing more efficient wind energy transfer to the ocean (Martin et al. 2014) and amplifying the Ekman transport. For instance, Williams and Carmack (2015) demonstrated the recent increase of yearly mean upwelling-favorable wind stresses over the open water compared to that over the ice-covered areas in the Canadian Beaufort Sea. Altogether, it implies that northeasterly winds together with a thinner ice cover may lead to amplified upwelling over the Mackenzie slope during all seasons and increase the availability of nutrients to the euphotic zone within the shelf system and thereby increase biological productivity, particularly in the open water season. This is consistent with direct observations of biological productivity along the shelf–slope environment (Tremblay et al. 2011) and throughout the circumpolar Arctic (Barber et al. 2015). Specifically, Spall et al. (2014) described the mechanism of vertical transport of nutrient-rich Pacific winter waters into the

surface layer under the upwelling-favorable wind conditions over the shallow Alaskan shelf. Authors also suggested that a combination of more frequent upwelling-favorable winds and reduced ice cover would result in a further increase in phytoplankton primary production.

Acknowledgments. This study was supported by the Canada Excellence Research Chair (CERC) program and Canada Research Chairs (CRC) program and conducted under the framework of the ArcticNet project Long-Term Observatories in Canadian Arctic Waters. This is a contribution of the Arctic Science Partnership (ASP).

REFERENCES

- Aagaard, K., and A. T. Roach, 1990: Arctic ocean-shelf exchange: Measurements in Barrow Canyon. *J. Geophys. Res.*, **95**, 18 163–18 175, doi:10.1029/JC095iC10p18163.
- Arctic Climatology Project, 1997: Environmental Working Group joint U.S.–Russian atlas of the Arctic Ocean—Winter period. National Snow and Ice Data Center, Boulder, CO, digital media. [Available online at <http://nsidc.org/data/g01961>.]
- , 1998: Environmental Working Group joint U.S.–Russian atlas of the Arctic Ocean—Summer period. National Snow and Ice Data Center, Boulder, CO, digital media. [Available online at <http://nsidc.org/data/g01961>.]
- Asplin, M. G., J. Lukovich, and D. Barber, 2009: Atmospheric forcing of the Beaufort Sea ice gyre: Surface pressure climatology and sea ice motion. *J. Geophys. Res.*, **114**, C00A06, doi:10.1029/2008JC005127.
- , D. Fissel, T. N. Papakyriakou, and D. G. Barber, 2015: Synoptic climatology of the southern Beaufort Sea troposphere with comparisons to surface winds. *Atmos.–Ocean*, **53**, 264–281, doi:10.1080/07055900.2015.1013438.
- Bakun, A., 1973: Coastal upwelling indices, west coast of North America, 1946–71. NOAA Tech. Rep. NMFS-SSRF-671, 103 pp.
- Barber, D. G., and J. M. Hanesiak, 2004: Meteorological forcing of sea ice concentrations in the southern Beaufort Sea over the period 1979 to 2000. *J. Geophys. Res.*, **109**, C06014, doi:10.1029/2003JC002027.
- , and Coauthors, 2015: Selected physical, biological and biogeochemical implication of a rapidly changing Arctic margin ice zone. *Prog. Oceanogr.*, **139**, 122–150, doi:10.1016/j.pocean.2015.09.003.
- Brugler, E. T., R. S. Pickart, G. W. K. Moore, S. Roberts, T. J. Weingartner, and H. Statscewich, 2014: Seasonal to interannual variability of the Pacific water boundary current in the Beaufort Sea. *Prog. Oceanogr.*, **127**, 1–20, doi:10.1016/j.pocean.2014.05.002.
- Cameron, M. W., 1953: Hydrographic and oceanographic observations in the Beaufort Sea, 1952. University of British Columbia Institute of Oceanography Progress Rep., 82 pp.
- Carmack, E., and E. A. Kulikov, 1998: Wind-forced upwelling and internal Kelvin wave generation in Mackenzie Canyon, Beaufort Sea. *J. Geophys. Res.*, **103**, 18 447–18 458, doi:10.1029/98JC00113.
- , and R. W. Macdonald, 2002: Oceanography of the Canadian shelf of the Beaufort Sea: A setting for marine life. *Arctic*, **55**, 29–45.

- , and D. C. Chapman, 2003: Wind-driven shelf/basin exchange on an Arctic shelf: The joint roles of ice cover extent and shelf-break bathymetry. *Geophys. Res. Lett.*, **30**, 1778, doi:10.1029/2003GL017526.
- Christensen, J. P., K. Shimada, I. Semiletov, and P. A. Wheeler, 2008: Chlorophyll response to shelf-break upwelling and winds in the Chukchi Sea, Alaska, in autumn. *Open Oceanogr. J.*, **2**, 34–53, doi:10.2174/1874252100802010034.
- Dmitrenko, I. A., J. A. Hoelemann, S. A. Kirillov, S. L. Berezovskaya, and H. Kassens, 2001: Role of barotropic sealevel changes in current formation on the eastern shelf of the Laptev Sea. *Dokl. Earth Sci.*, **377**, 243–249.
- , and Coauthors, 2010: Impact of the Arctic Ocean Atlantic water layer on Siberian shelf hydrography. *J. Geophys. Res.*, **115**, C08010, doi:10.1029/2009JC006020.
- , S. A. Kirillov, V. V. Ivanov, B. Rudels, N. Serra, and N. V. Koldunov, 2012: Modified halocline water over the Laptev Sea continental margin: Historical data analysis. *J. Climate*, **25**, 5556–5565, doi:10.1175/JCLI-D-11-00336.1.
- Estrade, P., P. Marchesiello, A. Colin De Verdiere, and C. Roy, 2008: Cross-shelf structure of coastal upwelling: A two-dimensional extension of Ekman's theory and a mechanism for inner shelf upwelling shut down. *J. Mar. Res.*, **66**, 589–616, doi:10.1357/002224008787536790.
- Falk-Petersen, S., V. Pavlov, J. Berge, F. Cottier, K. M. Kovacs, and Ch. Lydersen, 2015: At the rainbow's end: High productivity fueled by winter upwelling along an Arctic shelf. *Polar Biol.*, **38**, 5–11, doi:10.1007/s00300-014-1482-1.
- García-Reyes, M., J. L. Largier, and W. J. Sydeman, 2014: Synoptic-scale upwelling indices and predictions of phyto- and zooplankton populations. *Prog. Oceanogr.*, **120**, 177–188, doi:10.1016/j.pocean.2013.08.004.
- Garneau, M.-E., W. Vincent, L. Alonso-Saez, Y. Gratton, and C. Lovejoy, 2006: Prokaryotic community structure and heterotrophic production in a river-influenced coastal arctic ecosystem. *Aquat. Microb. Ecol.*, **42**, 27–40, doi:10.3354/ame042027.
- Gratton, Y., and Coauthors, 2012: Team 1: Physical oceanography. *On the Edge: From Knowledge to Action during the Fourth International Polar Year Circumpolar Flaw Lead Study*, D. Barber et al., Eds., Prolific Printing, 33–50.
- Hudak, D. R., and J. M. C. Young, 2002: Storm climatology of the southern Beaufort Sea. *Atmos.–Ocean*, **40**, 145–158, doi:10.3137/ao.400205.
- Jackson, J. M., H. Melling, J. V. Lukovich, D. Fissel, and D. G. Barber, 2015: Formation of winter water on the Canadian Beaufort shelf: New insight from observations during 2009–2011. *J. Geophys. Res. Oceans*, **120**, 4090–4107, doi:10.1002/2015JC010812.
- Lukovich, J. V., and D. G. Barber, 2006: Atmospheric controls on sea ice motion in the southern Beaufort Sea. *J. Geophys. Res.*, **111**, D18103, doi:10.1029/2005JD006408.
- Makhtas, A., D. Atkinson, M. Kulakov, S. Shutilin, R. Krishfield, and A. Proshutinsky, 2007: Atmospheric forcing validation for modeling the central Arctic. *Geophys. Res. Lett.*, **34**, L20706, doi:10.1029/2007GL031378.
- Martin, T., M. Steele, and J. Zhang, 2014: Seasonality and long-term trend of Arctic Ocean surface stress in a model. *J. Geophys. Res. Oceans*, **119**, 1723–1738, doi:10.1002/2013JC009425.
- Mathis, J. T., and Coauthors, 2012: Storm-induced upwelling of high p CO₂ waters onto the continental shelf of the western Arctic Ocean and implications for carbonate mineral saturation states. *Geophys. Res. Lett.*, **39**, L07606, doi:10.1029/2012GL051574.
- Moore, G. W. K., 2012: Decadal variability and a recent amplification of the summer Beaufort Sea high. *Geophys. Res. Lett.*, **39**, L10807, doi:10.1029/2012GL051570.
- Mundy, C. J., and Coauthors, 2009: Contribution of under-ice primary production to an ice-edge upwelling phytoplankton bloom in the Canadian Beaufort Sea. *Geophys. Res. Lett.*, **36**, L17601, doi:10.1029/2009GL038837.
- Pickart, R. S., G. W. K. Moore, D. J. Torres, P. S. Fratantoni, R. A. Goldsmith, and J. Yang, 2009: Upwelling on the continental slope of the Alaskan Beaufort Sea: Storms, ice, and oceanographic response. *J. Geophys. Res.*, **114**, C00A13, doi:10.1029/2008JC005009.
- , L. M. Schulze, G. W. K. Moore, M. A. Charette, K. R. Arrigo, G. Dijken, and S. L. Danielson, 2013a: Long-term trends of upwelling and impacts on primary productivity in the Alaskan Beaufort Sea. *Deep-Sea Res.*, **79**, 106–121, doi:10.1016/j.dsr.2013.05.003.
- , M. A. Spall, and J. T. Mathis, 2013b: Dynamics of upwelling in the Alaskan Beaufort Sea and associated shelf–basin fluxes. *Deep-Sea Res.*, **76**, 35–51, doi:10.1016/j.dsr.2013.01.007.
- Polyakov, I. V., and M. A. Johnson, 2000: Arctic decadal and interdecadal variability. *Geophys. Res. Lett.*, **27**, 4097–4100, doi:10.1029/2000GL011909.
- , and Coauthors, 2008: Arctic Ocean freshwater changes over the past 100 years and their causes. *J. Climate*, **21**, 364–384, doi:10.1175/2007JCLI1748.1.
- , and Coauthors, 2010: Arctic Ocean warming contributes to reduced polar ice cap. *J. Phys. Oceanogr.*, **40**, 2743–2756, doi:10.1175/2010JPO4339.1.
- Rigor, I. G., J. M. Wallace, and R. L. Colony, 2002: Response of sea ice to the Arctic Oscillation. *J. Climate*, **15**, 2648–2663, doi:10.1175/1520-0442(2002)015<2648:ROSITT>2.0.CO;2.
- Rodionov, S. N., J. E. Overland, and N. A. Bond, 2005: Spatial and temporal variability of the Aleutian climate. *Fish. Oceanogr.*, **14**, 3–21, doi:10.1111/j.1365-2419.2005.00363.x.
- Schulze, L. M., and R. S. Pickart, 2012: Seasonal variation of upwelling in the Alaskan Beaufort Sea: Impact of sea ice cover. *J. Geophys. Res.*, **117**, C06022, doi:10.1029/2012JC007985.
- Serreze, M. C., and A. P. Barrett, 2011: Characteristics of the Beaufort Sea high. *J. Climate*, **24**, 159–182, doi:10.1175/2010JCLI3636.1.
- Sévigny, C., Y. Gratton, and P. S. Galbraith, 2015: Frontal structures associated with coastal upwelling and ice-edge subduction events in southern Beaufort Sea during the Canadian Arctic Shelf Exchange Study. *J. Geophys. Res. Oceans*, **120**, 2523–2539, doi:10.1002/2014JC010641.
- Sorteberg, A., and J. E. Walsh, 2008: Seasonal cyclone variability at 70°N and its impact on moisture transport into the Arctic. *Tellus*, **60A**, 570–586, doi:10.1111/j.1600-0870.2008.00314.x.
- Spall, M. A., R. S. Pickart, P. S. Fratantoni, and A. J. Plueddemann, 2008: Western Arctic shelfbreak eddies: Formation and transport. *J. Phys. Oceanogr.*, **38**, 1644–1668, doi:10.1175/2007JPO3829.1.
- , —, E. T. Brugler, G. W. K. Moore, L. Thomas, and K. R. Arrigo, 2014: Role of shelfbreak upwelling in the formation of a massive under-ice bloom in the Chukchi Sea. *Deep-Sea Res. II*, **105**, 17–19, doi:10.1016/j.dsr2.2014.03.017.
- Spreen, G., R. Kwok, and D. Menemenlis, 2011: Trends in Arctic sea ice drift and role of wind forcing: 1992–2009. *Geophys. Res. Lett.*, **38**, L19501, doi:10.1029/2011GL048970.
- Stroeve, J. C., T. Markus, L. Boisvert, J. Miller, and A. Barrett, 2014: Changes in Arctic melt season and implications for sea ice loss. *Geophys. Res. Lett.*, **41**, 1216–1225, doi:10.1002/2013GL058951.

- Swift, J. H., K. Aagaard, L. Timokhov, and E. G. Nikiforov, 2005: Long-term variability of Arctic Ocean waters: Evidence from a reanalysis of the EWG data set. *J. Geophys. Res.*, **110**, C03012, doi:10.1029/2004JC002312.
- Thompson, D. W. J., and J. M. Wallace, 1998: The Arctic Oscillation signature in the wintertime geopotential height and temperature fields. *Geophys. Res. Lett.*, **25**, 1297–1300, doi:10.1029/98GL00950.
- Tremblay, J. E., and Coauthors, 2011: Climate forcing multiplies biological productivity in the coastal Arctic Ocean. *Geophys. Res. Lett.*, **38**, L18604, doi:10.1029/2011GL048825.
- Trenberth, K. E., and J. W. Hurrell, 1994: Decadal atmosphere-ocean variations in the Pacific. *Climate Dyn.*, **9**, 303–319, doi:10.1007/BF00204745.
- Tsimitri, C., and R. S. Pickart, 2006: Characterizing upwelling events in the western Arctic. *Eos, Trans. Amer. Geophys. Union*, **87** (Ocean Sciences Meeting Suppl.), Abstract OS350-08.
- Williams, B., and E. Carmack, 2015: The ‘interior’ shelves of the Arctic Ocean: Physical oceanographic setting, climatology and effects of sea-ice retreat on cross-shelf exchange. *Prog. Oceanogr.*, **139**, 24–41, doi:10.1016/j.pocean.2015.07.008.
- Williams, W. J., E. C. Carmack, K. Shimada, H. Melling, K. Aagaard, R. W. Macdonald, and R. G. Ingram, 2006: Joint effect of wind and ice motion in forcing upwelling in Mackenzie Trough, Beaufort Sea. *Cont. Shelf Res.*, **26**, 2352–2366, doi:10.1016/j.csr.2006.06.012.
- Wood, K. R., J. E. Overland, S. A. Salo, N. A. Bond, W. J. Williams, and X. Dong, 2013: Is there a “new normal” climate in the Beaufort Sea? *Polar Res.*, **32**, 19552, doi:10.3402/polar.v32i0.19552.
- Yang, J., 2009: Seasonal and interannual variability of downwelling in the Beaufort Sea. *J. Geophys. Res.*, **114**, C00A14, doi:10.1029/2008JC005084.
- Zhong, W., and J. Zhao, 2014: Deepening of the Atlantic Water core in the Canada Basin in 2003–11. *J. Phys. Oceanogr.*, **44**, 2353–2369, doi:10.1175/JPO-D-13-084.1.